Sample Overloading Effects in Polymer Characterization by Field-Flow Fractionation

KARIN D. CALDWELL, STEVEN L. BRIMHALL,* YUSHU GAO,† and J. CALVIN GIDDINGS,‡ *Department of Chemistry, University of Utah, Salt Lake City, Utah 84112*

Synopsis

There are two subtechniques of field-flow fractionation (FFF), thermal FFF and flow FFF, that have been successfully employed for polymer fractionation and characterization. These techniques are primarily analytical in nature, yielding accurate polymer characteristics from small sample loads ($\sim$ 10 μg or less, depending on detection sensitivity). In this study the effects of increasing sample size are examined. Modest increases in load are found to result in shifts toward higher retention volumes. These modest loads also result in some broadening of the sample peaks without a major loss of peak symmetry. Excessive loading, by contrast, appears to give rise both to skewed peaks and to new artifact peaks at higher levels of retention. These observations are discussed in terms of the concentration dependence of various properties (viscosity, diffusivity, thermal diffusivity) which influence polymer transport through the FFF channel. The results are used to indicate upper limits to suitable sample concentrations.

INTRODUCTION

Field-flow fractionation (FFF) is the generic term for a class of chromatographic-like separation techniques which, in addition to performing fractionation, permit the rather direct evaluation of certain important sample characteristics, such as molecular weight and diffusivity.[1-4] Separation, as in chromatography, is achieved along the axis of a flow channel, but retention is caused by an externally applied field, acting in a direction perpendicular to flow, which concentrates the sample against one of the channel walls (the accumulation wall). The velocity of migration of a species along the flow axis is strictly controlled by the resulting equilibrium concentration profile of that species near the accumulation wall. Species with less compressed profiles migrate faster than those with highly compressed profiles because molecules of the latter travel with the slow streamlines near the wall. It has been shown that these profiles are generally exponential in nature,[5] with the highest concentration at the accumulation wall and a thinning atmosphere of polymer extending in toward the center of the channel. The thickness of this atmosphere is characterized by the exponential constant l, which is essentially the mean elevation of polymer molecules above the wall. The observed level of retention is directly related to the characteristic thickness l, which in turn is a measure of some physical property of the sample, as discussed below.

*Current address: Dugway Proving Grounds, Dugway, Utah.
†Current address: Institute of Chemistry, Academia Sinica, Beijing, China.
‡To whom correspondence should be addressed.

Journal of Applied Polymer Science, Vol. 36, 703–719 (1988)
 CCC 0021-8995/88/030703-17$04.00

For small samples the concentration of sample material in the channel is dilute and the mean distance between component molecules is correspondingly large. Under these circumstances, each molecule acts essentially independently of each other molecule, which is a necessary condition for linear operation. As long as the behavior remains linear, the mean and variance of the elution time of component molecules (more generally, the detailed shape and position of the elution curve) remain independent of concentration. Linearity is strongly preferred for analytical work because of the simplicity of concentration-independent behavior. With linearity, one need only account for the interactions of the polymer molecule with the system and not with other polymer molecules.

One must guard against the onset of nonlinear conditions in FFF, particularly with polymeric samples. The reason is that the buildup of sample material near the accumulation wall in FFF heightens the concentration, thus endangering linearity. Polymeric molecules are particularly subject to chain entanglement and other interactive processes that lead to nonlinear behavior at only modest concentration.

Despite this background threat, it has been our experience that with reasonable care and good detector sensitivity, operation in the linear range is generally achievable. If, on the other hand, samples larger than the minimum detectable level are needed for subsequent analytical work or for reinjection into other FFF systems, the increase in concentration may seriously strain linearity. For this reason, we wish to better characterize the aberrations that occur in the transition from linear to nonlinear behavior.

In order to examine the nonlinear behavior of polymers in FFF, we have used high molecular weight linear polystyrenes as sample material in two different FFF systems. One is a thermal FFF system, in which the "field" is a temperature gradient imposed between the walls of the thin FFF channel. Here the concentration of polymer at the accumulation wall is due to thermal diffusion. The other is a flow FFF system, in which a cross-flow of carrier is established between semipermeable channel walls. The cross-flow serves to drive sample material to the accumulation wall. The comparison of these two systems is useful because they operate on the basis of the same general principles but are influenced by somewhat different physicochemical parameters, as will be shown explicitly below.

THEORY

In this section we will provide the background equations necessary to describe linear FFF, that is, FFF in the absence of overloading. This ideal case serves as a frame of reference from which departures due to overloading can be studied. No theory has yet been developed to describe overloading in FFF; such a theory would involve considerable complexity because of the simultaneous variation of concentration along both flow and field axes. Thus our treatment of overloading is limited to an examination of the nature of the perturbations superimposed on the reference frame of linear FFF.

Concentration Profile

Under the influence of an applied field or gradient, such as the temperature gradient in thermal FFF or the crossflow of liquid in flow FFF, an injected

sample will migrate toward one of the channel walls and accumulate there. This accumulation leads to an increased concentration near the wall and a depleted concentration over the remainder of the channel cross-section; it therefore has a profound effect on sample overloading.

The migration of sample material toward the accumulation wall is balanced by the dispersive effects of diffusion, leading to the rapid formation of a steady-state distribution. Once the steady-state condition is established, the concentration along transverse axis x can be expressed by the exponential form[7]

$$c(x, z) = c_o(z)\exp(-x/l) = c_o(z)\exp(-x/\lambda w) \tag{1}$$

where w is thickness of the channel and $\lambda = l/w$ is the retention parameter, a dimensionless measure of the thickness l of the sample zone in the x-direction. The magnitude of l and λ for a given component depends on the nature and strength of the applied field.

The term $c_o(z)$ in Eq. (1) is the sample concentration at the accumulation wall, located at $x = 0$. Generally the sample can be assumed to begin its migration in the channel distributed as a narrow plug along flow axis z, as illustrated in Figure 1. Under these conditions, $c_o(z)$ is a square function in the vicinity of the inlet at $z = 0$. Subsequently, $c_o(z)$ broadens into a Gaussian-like function.[2,3]

The highest possible level of magnification of the concentration of an injected sample of initial concentration c_{inj} is that found at the accumulation wall before any dilution is caused by band broadening. The equilibrium wall concentration $c_o(z)$ of such a zone is found by the integration of $c(x, z)$ in Eq. (1) over the full thickness w of the channel

$$\int_o^w c(x, z)\, dx = wc_{inj} \tag{2a}$$

which gives

$$c_o(z) = \frac{c_{inj}}{\lambda(1 - \exp(-1/\lambda))} \simeq \frac{c_{inj}}{\lambda} \tag{2b}$$

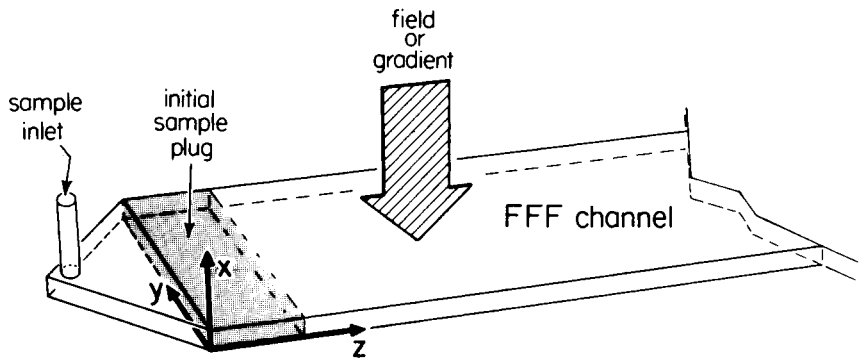

Fig. 1. Identification of the coordinate system of the FFF channel. A freshly injected sample slug (shaded area) is shown at the inlet end. Following relaxation of the sample into its equilibrium distribution, carrier is pumped along separation coordinate z, causing sample migration.

Since λ commonly falls in the range 0.01–0.1, this represents a substantial gain in concentration over the injected level c_{inj} prior to band broadening.

In the case of the two subtechniques considered here, the expressions for λ are well known.[3,4,8–10] For thermal FFF, λ is given to a good approximation by

$$\lambda_{\text{thermal}} = \frac{D}{D_T \Delta T} \tag{3}$$

where ΔT represents the temperature difference across the channel and D and D_T are the coefficients for ordinary and thermal diffusion, respectively. The ratio D/D_T is a function of sample molecular weight M. In a recent study[3] involving liner polystyrenes with M values ranging from 5×10^4 to 2×10^7 dissolved in tetrahydrofuran (THF), the product $\lambda \Delta T$, which approximately equals D/D_T according to Eq. (3), was found to vary with M according to

$$\log(\lambda \Delta T) = -0.53 \log M + 3.286 \tag{4}$$

This relationship can be assumed to illustrate the trend in λ with changes in M for other polymer-solvent systems as well.

Similarly, parameter λ for the flow FFF subtechnique is expressed as

$$\lambda_{\text{flow}} = DV^o/\dot{V}_c w^2 \tag{5}$$

where $\dot{V}_c$ is the volumetric cross-flowrate and V^o is the void volume of the channel. The relationship between diffusion coefficient D and sample molecular weight M depends on the solvent,[11] as does the relationship between D/D_T and M discussed above. Generally, $D = \text{const.}/\text{M}^b$, where $b \simeq 0.55$.

Retention

Experimental values of the retention parameter λ are obtained by measuring the retention volume V_r. The observed V_r is best expressed in terms of the corresponding retention ratio R by $R = V^o/V_r$, where V^o is the channel void volume. For most FFF systems, R is accurately related to λ as follows[1]

$$R = V^o/V_r = 6\lambda[\coth(1/2\lambda) - 2\lambda] \tag{6}$$

which approaches the limit

$$R = 6\lambda \tag{7}$$

for well-retained samples characterized by small values for R and λ. However, in the case of thermal FFF, the applied temperature gradient results in a gradient in viscosity across the channel; this causes a departure from the normally parabolic velocity profile in the channel and in Eq. (6), which is based on the parabolic assumption.[12] Fortunately, the present study is adequately served by retaining Eq. (6), which still provides a reasonable approximation under most experimental conditions.

Band Broadening

Since the band width reflects the degree of dilution of sample along the flow axis, it is a key element governing the degree of overloading. Band broadening in FFF, as in related chromatographic processes, is commonly expressed in terms of the plate height H. For a sample injected as a narrow pulse and subject to uniform migration, the plate height is given by the distance-based variance σ^2 of the eluting peak divided by the length L of the channel.[13] The additivity of variances makes it possible to express the total plate height as the sum of individual contributions.[13] In the field-flow fractionation of polymeric materials, the principal plate height components arise from nonequilibrium and sample polydispersity;[14] when large sample volumes are injected, the width of the injection slug will also affect the plate height.[15] Of these three, the variances caused by nonequilibrium[16] and sample polydispersity[14] continuously increase with the distance z migrated along the separation coordinate, whereas the variance resulting from the injection[15] represents a fixed contribution. All of these can be described explicitly in terms of system and sample parameters.[14]

Specifically, the variance due to the size of a square injection pulse (see Fig. 1) is given by

$$\sigma_{\text{inj}}^2 = \frac{1}{12}\left(\frac{V_{\text{inj}}L}{V^o}\right)^2 \tag{8}$$

where L and V^o represent the length and void volume of the channel and V_{inj} is the volume of the injected sample. The variance caused by mass transfer or nonequilibrium effects is expressed as

$$\sigma_{\text{neq}}^2 = \chi(\lambda)w^2\langle v\rangle Z/D \tag{9}$$

where Z is the downstream distance traveled by the center of the pulse and $\langle v\rangle$ is the mean velocity of carrier through the channel. The nonequilibrium coefficient χ is a known function of λ (16); in the limit of high retention the two are related by

$$\chi(\lambda) = 24\lambda^3 \tag{10}$$

The polydispersity contribution to variance, caused by the unequal migration rates of different components in a narrow sample, is described by[17]

$$\sigma_{\text{poly}}^2 = Z^2(d\ln V_r/d\ln M)^2(\mu - 1) \tag{11}$$

where μ is the polydispersity index, the ratio of weight to number average molecular weight.

The total variance of the migrating zone is given by the sum of the three variances above

$$\sigma^2 = \sigma_{\text{inj}}^2 + \sigma_{\text{neq}}^2 + \sigma_{\text{poly}}^2 \tag{12}$$

providing all other contributions to band broadening are negligible.

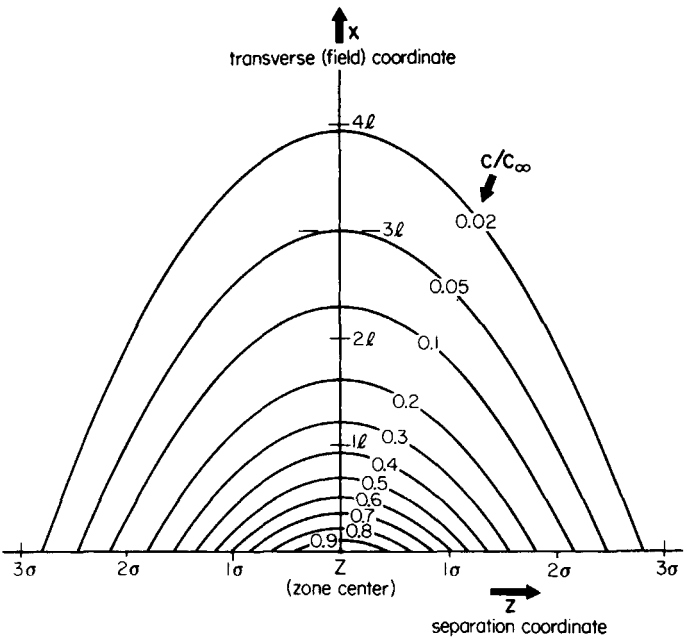

Fig. 2. Ideal distribution of a polymer component in an FFF channel (i.e., after assuming an exponential distribution in the field direction and a Gaussian distribution along the separation coordinate). The curves join volume elements of identical concentration. The indicated concentrations, c/c_{oo}, represent actual concentrations normalized by c_{oo}, the maximum concentration of the zone found at the accumulation wall in the zone's center. The z-axis is graduated in standard deviations and the x-axis is graduated in multiples of average layer thickness $l = \lambda w$.

Shortly after injection, the narrow zone is assumed to broaden into a Gaussian concentration profile along flow coordinate z. Since Eq. (1) specifies an exponential distribution in the x-direction, the resulting two-dimensional concentration is[7]

$$c(x, z) = c_{oo}\exp\left[-(z - Z)^2/2\sigma^2\right]\exp(-x/\lambda w) \tag{13}$$

where c_{oo} is the maximum concentration in the zone, found at the wall ($x = 0$) and in the center ($z = Z$) of the Gaussian distribution. This two-dimensional distribution is plotted in Figure 2 as lines of constant concentration. Integration of the distribution over the spatial coordinates of the zone, including over coordinate y from zero to breadth b, gives the total amount of sample m' injected into the channel

$$m' = c_{oo}(2\pi\sigma^2)^{1/2}bw\lambda\left[1 - \exp(-1/\lambda)\right] \simeq c_{oo}(2\pi\sigma^2)^{1/2}bw\lambda \tag{14}$$

where σ^2 is the total zone variance given by Eq. (12). Replacing m' by the product of the injected sample volume V_{inj} and sample concentration c_{inj} and writing the product of channel breadth b and thickness w as the cross-sectional area V^o/L, we obtain the following expression for the maximum zonal concentration

$$c_{oo} = \frac{V_{inj}c_{inj}L}{(2\pi\sigma^2)^{1/2}V^o\lambda\left[1 - \exp(-1/\lambda)\right]} \simeq \frac{V_{inj}c_{inj}L}{(2\pi\sigma^2)^{1/2}V^o\lambda} \tag{15}$$

We note that c_{oo} varies inversely with σ, which in turn varies with the position Z of the zone center as expressed in Eqs. (9) and (11).

Overloading Phenomena

A number of relevant transport coefficients are strongly affected as the concentration of polymer increases from its infinite dilution level. The altered transport coefficients lead to changes in mean transport rates and thus in retention ratio R. Also, the fact that these coefficients vary from one position to another in response to concentration variations in the zone means that the zone becomes distorted relative to its ideal (Gaussian) configuration in the course of migration. These disturbances will be elaborated below.

Three transport parameters are particularly important for the systems discussed here: viscosity η, diffusion coefficient D, and thermal diffusion coefficient D_T. The first of these affects the detailed flow profile and the other two are involved in zone formation and migration through their influence on λ as reflected by Eqs. (3) and (5). It is well known that η and D are increased and decreased, respectively, with increases in concentration. The influence of concentration on D_T is uncertain.

Polymeric material is carried downstream in FFF by the motion of fluid layers near the wall. The velocity of a small patch of polymer-containing fluid in the wall region is strongly affected by viscosity, being roughly inversely proportional to the mean solution viscosity at that point. The increase in viscosity with mean concentration is therefore expected to retard the downstream motion of the polymeric material, thus increasing retention time and volume and reducing R. At the same time, viscosity variations will lead to zone distortion because at the center of the zone (at $z = Z$), where the concentration is greatest, the retardation is also at its maximum. For this reason the front and rear regions of a zone will tend to outrace the center. The rear of the zone will thus pile into the center and form a sharper boundary than in the case of linear FFF. However, the frontal region will move increasingly in advance of the central region, stretching the zone out toward the leading edge. Consequently, we expect viscosity effects, when sufficiently large, to lead to zone distortion involving an elongated front on otherwise narrow polymer bands. This phenomenon is expected to influence all forms of FFF when operated at high concentration levels.

Diffusivity D is also widely involved in overloading effects. The l and λ values in both thermal and flow FFF are proportional to D as shown by Eqs. (3) and (5). This means that the depression of D by overloading leads to a reduced migration velocity. This phenomenon has the same general consequence as the viscosity changes noted earlier: zone migration velocity will generally fall off with increasing concentration and the zone will become more and more distorted with a "fronting" asymmetry.

Changes in D also affect band broadening as shown in Eq. (9). However, the effects are not clear cut because the direct changes in D will be accompanied by changes in λ, as just noted.

Other overloading effects relate more specifically to individual methods. In thermal FFF any change in D_T with concentration will influence λ, as indicated in Eq. (3). In flow FFF high zonal concentrations will locally reduce

the velocity of the crossflow stream, which will increase λ because the crossflow is responsible for compressing the polymer layer in the first place. This phenomenon will have an effect opposite to that of viscosity and diffusivity, leading to an increase in migration rate with increasing concentration, thus spawning tailing peaks.

EXPERIMENTAL

The flow FFF system used in this work was constructed of stainless steel, as has been described elsewhere.[4] The channel walls are fritted steel with 35 μm nominal pore size; the resulting wall permeability is necessary to establish a cross-flow. The accumulation wall was covered by a cellulose nitrate membrane of type EI 41 from Schleicher and Schuell, Inc. The channel dimensions were established by a Teflon spacer whose thickness (dimension w) was 0.0532 cm and from which a section of tip-to-tip length 41.6 cm (dimension L) and breadth 1.95 cm (dimension b) was cut and removed. The measured void volume V^o of the resulting channel was 3.9 mL, a value somewhat smaller than the geometrical volume.

Two Cheminert metering pumps from Chromatronix Inc. were used to supply the axial flow and the cross-flow. The effluent from the channel (axial flow) was regulated with an in-house built syringe pump (unpump) operated in reverse. The effluent was monitored by a Multiref 902 refractive index detector from Optilab (Vallingby Sweden) whose signal was fed to an Omniscribe chart recorder from Houston Instruments. Injections were made by syringe directly onto the channel; a period of stopped axial flow followed the injection to eliminate zone broadening due to relaxation effects.

The thermal FFF system used here has also been described elsewhere.[3] Its channel geometry is defined by a 0.0254 cm thick mylar spacer from which a section 2.0 cm in breadth and 47 cm long was cut and removed. This spacer was sandwiched between two chrome-plated copper blocks whose highly polished surfaces form the channel walls. The upper block was heated by two 1.5 kW cartridge heaters while the lower block was cooled by running tap water. Carrier was delivered to this system by means of a pneumatic pump.[18] The effluent was routed through an Altex UV detector from Beckmann Instruments which monitored absorbance at 254 nm. The detector response was recorded on a flatbed recorder of type Goertz Metrawatt.

The carriers were ethylbenzene in the case of flow FFF and tetrahydrofuran for thermal FFF. Both solvents were reagent grade and were obtained from Fisher Scientific Corporation. The samples used in both systems were linear polystyrenes; molecular weights, polydispersities, and suppliers are listed in Table I.

TABLE I
Polystyrene Samples Used in the Study of Overloading Effects

M (dalton)	Polydispersity ($\mu = M_W/M_N$)	Supplier
860,000	1.15	ARRO Laboratories, Inc.
670,000	1.15	Pressure Chemical Co.
411,000	1.10	Mann Research Labs, Inc.
200,000	< 1.06	Pressure Chemical Co.

RESULTS AND DISCUSSION

We first examine overall changes in migration velocity with increasing sample load. To this end, Figure 3 has been plotted to show the variation of R with respect to m' for a number of thermal and flow FFF runs. The retention volume used to calculate R is measured at the maximum height of the respective peaks. The magnitude of R is shown relative to its value at infinite dilution R_∞. These relative migration velocities are in most cases seen to fall off with increasing sample size, as expected from the known effects of increasing sample concentration on viscosity and diffusivity noted earlier. The maximum concentration c_{oo} in the migrating zone is seen from Eq. (15) to vary linearly with the injected amount of sample m' ($= V_{inj} c_{inj}$). An increase in either the volume of the injection slug (V_{inj}) or the concentration of sample (c_{inj}) is therefore expected to result in the reduced migration velocities observed in Figure 3.

In addition to these effects, Eq. (15) predicts c_{oo} to vary inversely with retention parameter λ. A decrease in λ, resulting from an increased compression of the sample layer at the accumulation wall (i.e., increased retention), can therefore be expected to cause the same type of concentration-induced nonidealities as those observed at high sample loads. A demonstration of this effect is seen in Figure 4, where identical amounts ($V_{inj} = 50$ μL, $c_{inj} = 20$ mg/mL) of three linear polystyrene samples were studied by varying the crossflow in flow FFF. Equations (5) and (6) were then used to convert the observed retentions into apparent diffusion coefficients to be recorded as functions of $1/R$. This parameter is roughly proportional to $1/\lambda$, according to Eq. (7), and is consequently related to c_{oo}. However, from Eqs. (9), (11), and

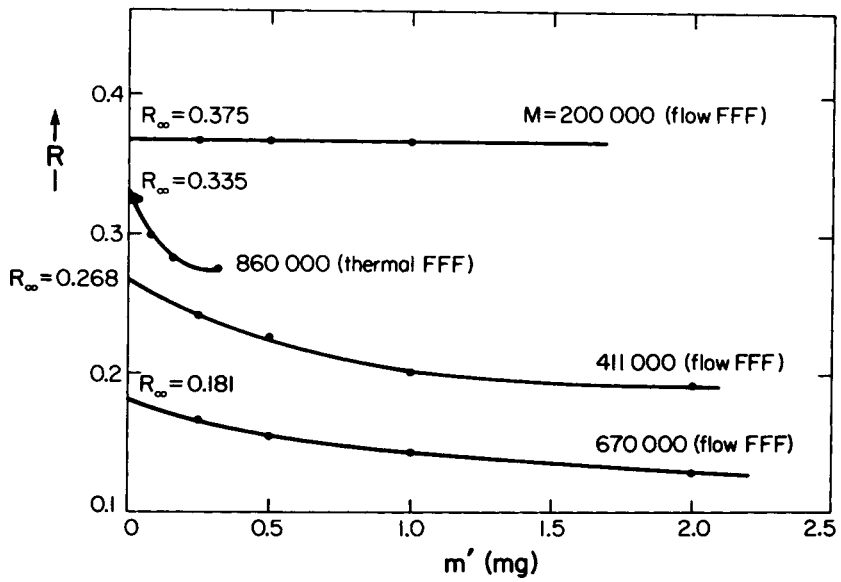

Fig. 3. Variation of retention ratio R with amount m' of injected polystyrene sample. For the thermal FFF plot, M = 860,000, ΔT = 25°C and cold wall temperature T_c = 15°C. For flow FFF there are three plots for M = 200,000, 411,000, and 670,000, respectively. For these the crossflow was held constant at 20 mL/h.

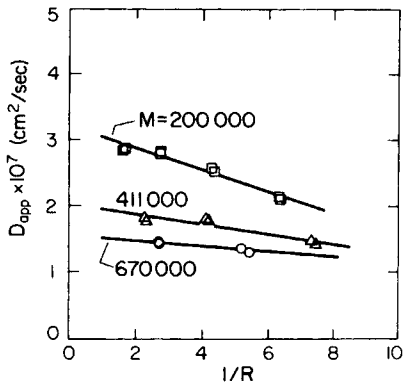

Fig. 4. Retention-derived apparent diffusion coefficients for three linear polystyrene samples obtained through flow FFF experiments using ethylbenzene as carrier. The amount of sample injected (1 mg) was identical in all cases (V_{inj} = 50 μL, c_{inj} = 20 mg/mL). V^o = 3.9 mL and w = 0.0532 cm.

(12) it is evident that changes in R will also result in variations in the zone width σ which, in turn, affects c_{oo}.

Figures 3 and 4 demonstrate the need in careful analytical work for measuring retention-derived parameters (such as D) under a variety of experimental conditions, and extrapolating these apparent parameters to zero c_{inj} in order to determine their ideal values at infinite dilution.

Many of the fractograms used to compile Figures 3 and 4 showed elution peaks with significant fronting. The flow FFF fractograms of Figure 5 (used to obtain results shown in Figure 4) clearly demonstrate this effect for the larger samples sizes, which is an expected consequence of the increased viscosity and decreased diffusivity associated with concentrated zones, as noted above. (Apparently the reduction of crossflow in the sample region, which would show an opposite trend, is a lesser effect.) The influence of concentration on the viscosity of these polystyrene samples will be discussed further below.

Both the load-induced fronting and shifts to higher retention times are also observed in the thermal FFF fractograms of Figure 6, which were recorded under constant field (temperature drop = 25°C) but with varying amounts of sample originating from stock solutions of different concentration. There is a qualitative agreement between the peak shapes of Figure 5 and those from the low concentration runs of Figure 6(a). However, significant departures from the Figure 5 cases are noted by the appearance of subsidiary peaks in the tails of those peaks which result from injections of the more concentrated samples [Figs. 6(b) and (c)]. Although extraneous peaks are always seen in fractograms of these highly concentrated samples, their size and shape are highly irreproducible.

The emergence of new peaks with high retention times suggests the possible presence of relatively stable aggregates or microgels of high apparent molecular weight.[19,20] The injection of 320 μg polystyrene (M 860,000) from a stock solution with concentration 1 mg/mL [Fig. 6(a)] fails to produce evidence of this type of species, whereas an injection of 125 μg of the same polymer from a stock solution with concentration 25 mg/mL gives rise to a substantial

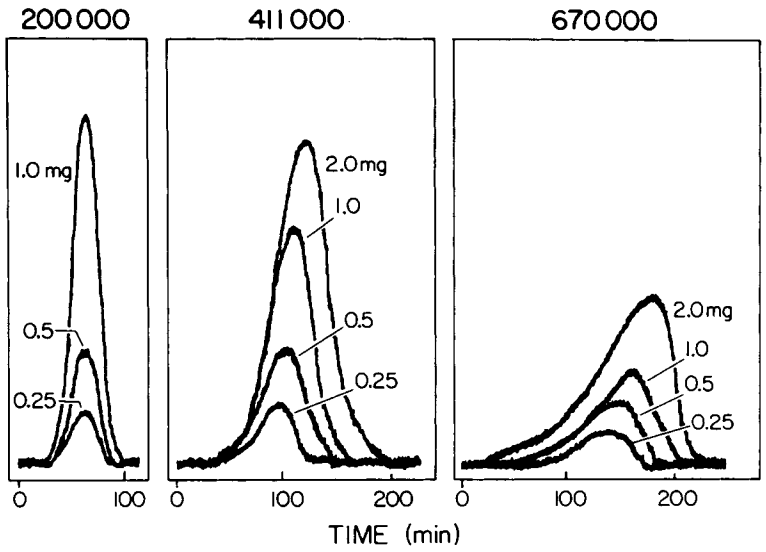

Fig. 5. Fractograms for different polystyrene molecular weights using flow FFF at a constant cross flowrate of 20 mL/h and a channel flowrate of 10 mL/h. Injected sample concentration was 20 mg/mL. The effects of overloading, both peak fronting and shifts in retention time or volume, are most pronounced for the sample of highest molecular weight, whose distribution is most compressed and whose molecules are generally most susceptible to chain entanglement.

secondary peak [Fig. 6(c)], possibly due to such polymer aggregates. It is clear that the different levels of concentration induce substantial differences in the form and distribution of the migrating sample.

An explanation for this behavior may be found in the tendency for polymer solutions to undergo a rather abrupt transition from "dilute" to "semidilute" behavior at some critical concentration c^*. The magnitude of c^* has been shown to depend as follows on the polymer's molecular weight M and radius of gyration $\langle r \rangle$, as well as on the density ρ of the solvent[21,22]

$$c^* = M/N_A \rho \langle r \rangle^3 \tag{16}$$

Here N_A represents Avogardro's number. Clearly, the critical concentration for a given polymer-solvent system reflects the goodness of the solvent, as $\langle r \rangle$ is known to increase with increased solvation of the macromolecule. The following empirical relationship between $\langle r \rangle$ and M has been found to hold for linear polystyrene in good solvents[21]

$$\langle r \rangle = 1.45 \times 10^{-9} M^{0.595} \tag{17}$$

Although the above relationship was established for the solvent benzene, it is expected to reasonably describe the behavior of polystyrene in other good solvents, such as THF used here. From a combination of Eqs. (16) and (17) one finds an explicit relationship between c^* (in g/g solution), ρ, and M

$$c^* = 575 \rho^{-1} M^{-0.785} \tag{18}$$

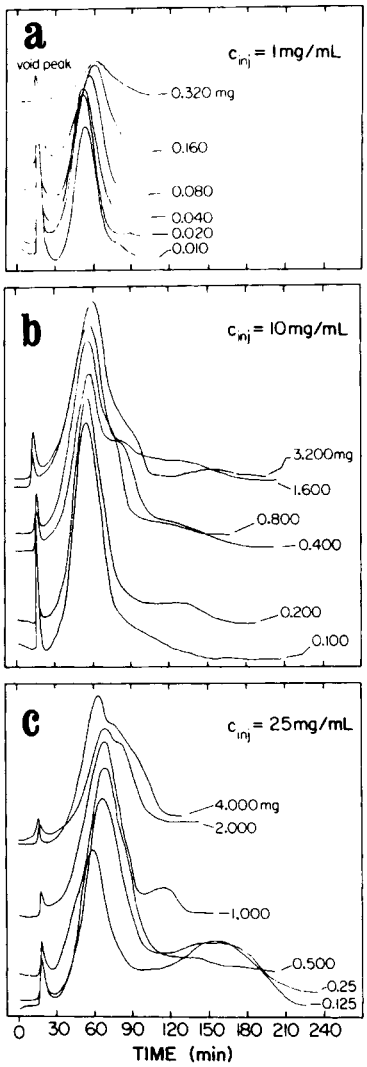

Fig. 6. Fractograms from thermal FFF for polystyrene with M = 860,000 in THF. The temperature drop was held constant at 25°C with the cold wall at 288 K. (a) The sample concentration c_{inj} was 1 mg/mL and injection volumes V_{inj} varied from 10 μL to 320 μL. (b) The sample concentration c_{inj} was 10 mg/mL and injection volumes V_{inj} varied from 10 μL to 320 μL. (c) The sample concentration c_{inj} was 25 mg/mL and V_{inj} was varied from 5 μL to 160 mL.

Transport properties, such as diffusivity D and viscosity η, undergo rapid changes in the vicinity of c^*. According to DeGennes,[23] the semidilute region ($c > c^*$) for solutions of a polymer with molecular weight M and concentration c is characterized by the following relationships

$$D = AM^{-2}c^{-1.75} \tag{19}$$

and

$$\eta = BM^{3}c^{3.75} \tag{20}$$

where A and B are constants. The strong effect of concentration on D and η in the semidilute regime is in marked contrast to dilute solution behavior, which is generally well described by just a second-order perturbation due to concentration.[24] Therefore, abnormal retention behavior can be anticipated if any significant portion of a zone is present as a semidilute solution.

To examine this matter further, we assume (as stated previously) that the zone is injected as a square plug (see Fig. 1) whose contents rapidly relax to an exponential distribution in the x-direction. As the channel flow begins to transport the zone downstream, a variety of zone-broadening mechanisms come into play which contribute to the dilution of the sample and the eventual formation (ideally) of a Gaussian distribution along the z-direction. The maximum concentration c_{oo} within this Gaussian zone [see Eq. (13)] will be less than the initial wall concentration of $c_o(0)$ of the square plug because of dilution. Consequently, for any FFF experiment, $c_o(0)$ is the highest concentration. To keep $c_o(0)$ within fixed limits, such as $c_o(0) < c^*$, the selection of a suitable sample concentration, c_{inj}, must be made from Eq. (2b). Figure 7 shows the maximum concentration of polystyrene in benzene allowed by this criterion as a function of molecular weight M and retention ratio R. The figure is compiled using Eqs. (2b) and (6) to yield $c_o(0)$ for a given R and Eq. (18) to estimate c^* for a given M.

The fractograms of Figure 6 were all obtained for a polystyrene sample of molecular weight 860,000 in THF. Each of individual Figures 6(a), (b), and (c) reflects the results of variations in V_{inj} for a constant c_{inj}; the values of c_{inj} in the three cases were 1 mg/mL, 10 mg/mL, and 25 mg/mL, respectively. The difference between the fractograms in Figure 6(a) and those of 6(b) and 6(c)

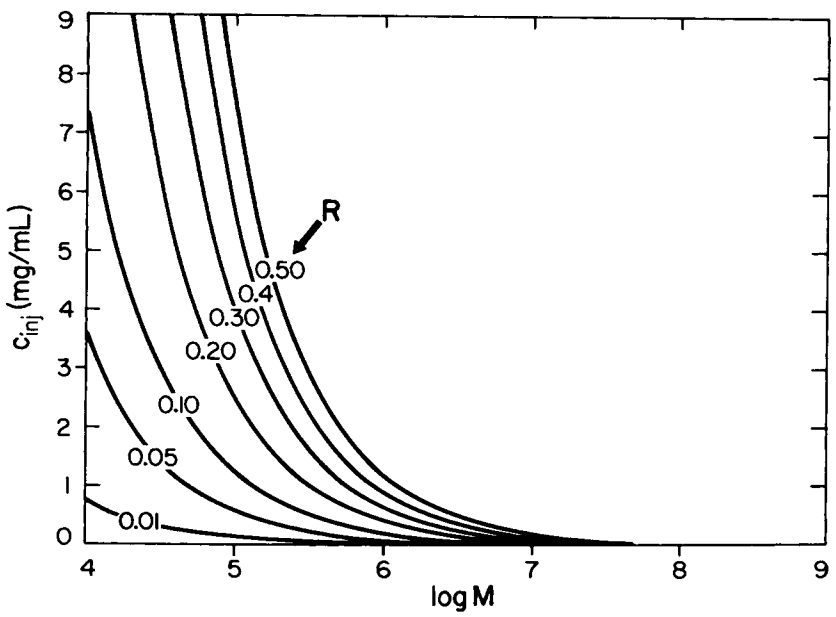

Fig. 7. Dependence on sample molecular weight M of the maximum sample concentration c_{inj} which can be injected at given levels of retention (represented by retention ratio R) without forcing any portion of the zone to exceed c^*.

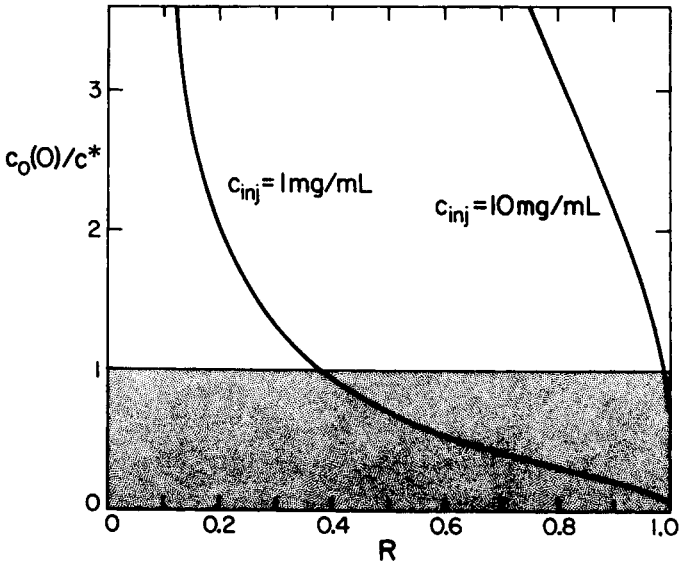

Fig. 8. Relationship between wall concentration $c_o(0)$ and retention ratio R for different injected concentrations of a linear polystyrene sample with M = 860,000. The wall concentration is normalized through division with c^* to highlight levels of retention suitable for work with the stock solutions which were used to generate Figure 6.

may be explained by Figure 8, which shows the influence of retention ratio R on the ratio $c_o(0)/c^*$ for different concentrations of the 860,000 dalton polystyrene. A sample concentration of 1 mg/mL is seen to leave the zone in a dilute state for $0.375 < R < 1$. Although the temperature drop in the actual experiment (25°C) gave an R value of 0.325, which translates into a larger retention volume than the critical value of $R = 0.375$ (for which $c_o(0) = c^*$), the inevitable dilution of the sample during the injection may have contributed to keep the entire zone in a dilute, as opposed to a semidilute, state throughout all the experiments of Figure 6(a). By contrast, a sample concentration of 10 mg/mL, as was used in Figure 6(b), brings part of the zone into a semidilute state even at an R of 0.99, which implies a retention ratio well above the anticipated level ($R = 0.325$). The sample concentration of 25 mg/mL, used in Figure 6(c), is already far in excess of c^* for this polymer ($\simeq$ 13 mg/mL).

By concentrating the polymer sample at the accumulation wall, one increases the viscosity across the zone, which in turn results in a reduced migration velocity, as noted earlier. Figure 9 illustrates the effect of polymer concentration on the viscosity of solutions containing the 860,000 dalton polystyrene sample of Figure 6. The curve was assembled from intrinsic viscosity data[25] for this sample in dilute solution, in combination with Eq. (20) which describes its semidilute regime. This diagram indicates that strong viscosity effects are indeed present in zones with significant semidilute behavior.

A comparison of the three parts of Figure 6 lends experimental support to the premise that low sample concentrations are desirable in terms of reducing nonideal behavior of the zone during fractionation.

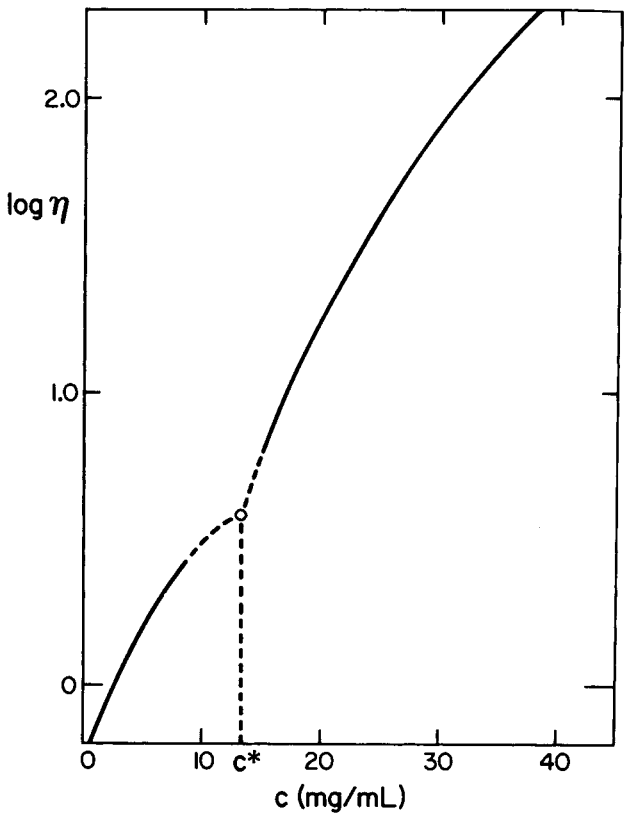

Fig. 9. Relationship between viscosity η (expressed in centipoise) and concentration c for a solution of linear polystyrene of M = 860,000 in THF. The curve has two branches which were forced to coincide at the system's critical concentration (13.3 mg/mL). Below c^* the viscosity is assumed to follow a relationship based on the intrinsic viscosity given in Ref. 25, in conjunction with Eqs. (23-6) of Ref. 6: $\eta = 0.54 + 1.3374c + 1.1593c^2$ (c in g/dL); above c^*, the dependence of viscosity on c is given by Eq. (20).[23]

In work with large samples one faces the choice of injecting either a small sample volume (V_{inj}) at high concentration (c_{inj}), or a larger volume at low concentration. The advantage of the former approach would derive from the smaller zone broadening associated with a small V_{inj}, as seen from Eq. (8). In light of the above evidence, however, the high sample concentrations required for this approach may introduce unwanted nonidealities into the fractionation. While the latter approach may result in a certain loss of resolution due to the larger sample volume, the gains in terms of sample behavior at low c_{inj} may be substantial.

Table II is a compilation of the levels of zone broadening expected from the three contributions to dispersion listed in Eq. (12). Both σ^2_{neq} and σ^2_{poly} are functions of retention; the table lists values for these terms calculated from Eqs. (9) and (11) for a series of values of the retention parameter λ. The calculations are all made for an 860,000 dalton polystyrene with an assumed diffusion coefficient[21] of 1.18×10^{-7} cm^2/s and a μ ($= \overline{M}_w/\overline{M}_n$) of 1.15. For comparison, the table also lists zone variances for a hypothetical sample of

TABLE II
Contributions to Zone Variance at Different Levels of Retention Ratio R of 860,000 Molecular Weight Polystyrene in Benzene*

			Monodisperse ($\mu = 1.0$, $\sigma^2_{poly} = 0$)			Polydisperse ($\mu = 1.15$)	
R	λ	V_{inj} (μL)	σ^2_{inj} (cm^2)	σ^2_{neq} (cm^2)	σ^2_{tot} (cm^2)	σ^2_{poly} (cm^2)	σ^2_{tot} (cm^2)
1	∞	10	0.004	200.7	200.7	0	200.7
		100	0.348		201.0		201.0
		250	2.125		202.9		202.9
0.50	0.1056	10	0.004	194.9	194.9	43.20	238.1
		100	0.348		195.2		238.4
		250	2.175		197.0		240.2
0.25	0.0459	10	0.004	32.29	32.29	65.41	97.7
		100	0.348		32.64		98.05
		250	2.175		34.47		99.88
0.10	0.0173	10	0.004	2.26	2.26	75.25	77.51
		100	0.348		2.61		77.86
		250	2.175		4.44		79.69
0.05	0.0085	10	0.004	0.28	0.28	78.17	78.45
		100	0.348		0.63		78.80
		250	2.175		2.46		80.63
0.01	0.00167	10	0.004	0.002	0.006	80.90	80.91
		100	0.348		0.350		81.25
		250	2.175		2.177		82.98

*Parameters used in establishing this table are: $V^0 = 2.3$ mL, $w = 0.0254$ cm, $b = 2.0$ cm, $\langle v \rangle = 0.082$ cm/s (15 mL/h), $D = 1.18 \times 10^{-7}$ cm^2/s. Equations (8), (9), and (11) were used to calculate σ^2_{inj}, σ^2_{neq}, and σ^2_{poly}, respectively.

zero polydispersity. The table shows that even large injection volumes (250 μL is in excess of 10% of the channel volume) contribute insignificantly to the bandwidth at a low to modest retention volume (relatively large R) of a monodisperse sample. Only for retentions of more than ten column volumes ($R < 0.1$) is this injection contribution comparable to, or larger than, the nonequilibrium contribution under the assumed experimental conditions. Polydisperse samples, in turn, undergo significant band broadening as a result of the fractionation of their various components. This broadening reflects the molecular weight distribution (MWD) of the sample, making it possible to calculate the MWD from the elution profile.[17]

CONCLUSION

Although field-flow fractionation is an analytical technique which performs most accurately at low sample loads, it has been shown to be applicable to the fractionation of moderate quantities (of the order of 0.5–1 mg) of high molecular weight polymer in a single run. These amounts appear to be best processed as injections of large volumes of dilute sample, since high sample concentrations are more likely to lead to nonideal behavior. If the desired resolution permits, it is advisable to perform the fractionation at low retention volumes where moderate compression of the zones keeps nonidealities at a minimum. This condition may conflict with the use of programmed (time-

dependent) field changes,[26,27] a method which is otherwise conveniently applied in order to shorten separation times.

Whenever FFF retention data are to be used for the accurate characterization of sample molecular weights or diffusivities, it is appropriate to vary both sample concentration and the level of retention until the chosen characteristic remains invariant with experimental conditions.

This work was supported by Grant No. CHE-8218503 from the National Science Foundation.

References

1. J. C. Giddings, *Pure Appl. Chem.*, **51**, 1459 (1979).
2. J. C. Giddings, K. A. Graff, K. D. Caldwell, M. N. Myers, *Advances in Chemistry Series*, No. 203, C. D. Craver, Ed., American Chemical Society, Washington DC, 1983, p. 257.
3. Y. S. Gao, K. D. Caldwell, M. N. Myers, and J. C. Giddings, *Macromolecules*, **18**, 1272 (1985).
4. S. L. Brimhall, M. N. Myers, K. D. Caldwell, and J. C. Giddings, *J. Polym. Sci., Polym. Lett. Ed.*, **22**, 339 (1984).
5. M. E. Hovingh, G. H. Thompson, and J. C. Giddings, *Anal. Chem.*, **42**, 195 (1970).
6. C. Tanford, *Physical Chemistry of Macromolecules*, Wiley, New York, 1961, Chap. 6.
7. J. C. Giddings, F. J. F. Yang, and M. N. Myers, *Anal. Chem.*, **46**, 1917 (1974).
8. J. C. Giddings, F. J. Yang, and M. N. Myers, *Anal. Chem.*, **48**, 1126 (1976).
9. M. N. Myers, K. D. Caldwell, and J. C. Giddings, *Sep. Sci.*, **9**, 47 (1974).
10. J. C. Giddings, K. D. Caldwell, and M. N. Myers, *Macromolecules*, **9**, 106 (1976).
11. P. J. Flory, *Principles of Polymer Chemistry*, Cornell University Press, Ithaca, NY, 1953, Chap. 14.
12. J. J. Gunderson, K. D. Caldwell, and J. C. Giddings, *Sep. Sci. Technol.*, **19**, 667 (1984).
13. J. C. Giddings, *Dynamics of Chromatography*, Dekker, New York, 1965.
14. L. K. Smith, M. N. Myers, and J. C. Giddings, *Anal. Chem.*, **49**, 1750 (1977).
15. J. C. Giddings, G. Karaiskakis, and K. D. Caldwell, *Sep. Sci. Technol.*, **16**, 725 (1981).
16. J. C. Giddings, Y. H. Yoon, K. D. Caldwell, M. N. Myers, and M. E. Hovingh, *Sep. Sci.*, **10**, 447 (1975).
17. M. E. Schimpf, M. N. Myers, and J. C. Giddings, *J. Appl. Polym. Sci.*, **33**, 117 (1987).
18. J. C. Giddings, M. Martin, and M. N. Myers, *J. Chromatogr.*, **158**, 419 (1978).
19. H.-M. Tan, A. Moet, A. Holtner, and E. Baer, *Macromolecules*, **16**, 28 (1983).
20. P. T. Callaghan and D. N. Pinder, *Macromolecules*, **13**, 1085 (1980).
21. M. Adam and M. Delsanti, *Macromolecules*, **10**, 1229 (1977).
22. K. Kubota, K. M. Abbey, and B. Chu, *Macromolecules*, **16**, 137 (1983).
23. P. G. DeGennes, *Macromolecules*, **9**, 594 (1976).
24. W. Mandema and H. Zeldenrust, *Polymer*, **18**, 835 (1977).
25. W. W. Yau, J. J. Kirkland, and D. D. Bly, *Modern Size Exclusion Liquid Chromatography*, 1st ed., Wiley, New York, 1979, p. 336.
26. J. C. Giddings, L. K. Smith, and M. N. Myers, *Anal. Chem.*, **48**, 1587 (1976).
27. J. C. Giddings and K. D. Caldwell, *Anal. Chem.*, **56**, 2093 (1984).

Received July 13, 1987
Accepted October 12, 1987